Mitolidis, G. J., Salonikios, T. N. & Kappos, A. J. (2012). Test results and strength estimation of R/C beams strengthened against flexural or shear failure by the use of SRP and CFRP. Composites Part B: Engineering, 43(3), pp. 1117-1129. doi: 10.1016/j.compositesb.2011.11.034

CITY UNIVERSITY LONDON

EST 1894

City Research Online

Test Results and Strength Estimation of R/C Beams Strengthened Against Flexural or Shear Failure by the Use of SRP and CFRP

George J. Mitolidis[a], Thomas N. Salonikios[b], Andreas J. Kappos[a]

[a]*Aristotle University of Thessaloniki, Laboratory of concrete and Masonry Structures, Thessaloniki, Greece*

[b] *Institute of Engineering Seismology and Earthquake Engineering, Agiou Georgiou 5, Patriarchika, Pylaia, 55535 Thessaloniki Greece*

Abstract

The paper reports tests on three groups of reinforced concrete (R/C) beam full-scale specimens, strengthened in flexural or shear using Steel Reinforced Polymers (SRP) and Carbon Fibre Reinforced Polymers (CFRP). The first group of five specimens represents the middle part of the span of a continuous beam and specimens are flexurally strengthened. The second group represents the support region of a continuous beam and its four specimens are strengthened in flexure. The third group also represents the support region of a continuous beam and its four specimens are strengthened in shear. Four specimens in total are tested unstrengthened to allow comparisons with the response of strengthened specimens. In addition to the different part of the beam that each specimen represented and the shear or flexural strengthening, the main parameters that varied among the specimens were: the type of polymer (SRP of two different types, or CFRP), the type of steel bars (ribbed or smooth, the latter being representative of older R/C members), the type of anchorage used for the polymers, and the way loading is applied to the specimens. Low strength concrete grade is used for the specimens, again to simulate older R/C members. The recorded response of the specimens is presented and discussed, and the experimentally measured strengths of the specimens are estimated analytically on the basis of the measured deformations of the specimens. Finally conclusions are drawn regarding the relative performance and merits of SRPs and CFRPs as strengthening materials for R/C beams.

Keywords: A. Polymer-matrix composites (PMCs), B. Flexural Strengthening, Shear strengthening, C. Strength analytical calculations, D. Experimental Testing.

1. Introduction

The properties of SRPs and the feasibility of using such materials in strengthening of R/C structural members were studied over the last decade by various research groups around the world. Direct tension tests of these materials (steel fibres/cords embedded in polymeric resin) have shown a small capacity for inelastic deformation [1], [2] that differentiates them from FRPs that fail in a brittle way. It was also found that the properties of SRPs, i.e. tensile strength, modulus of elasticity, and

Poisson ratio can be determined using the equations of micromechanics, with the exception of the modulus of elasticity perpendicular to the direction of fibres [3]. Comparative tests involving steel wire cords embedded in either polymeric resin (SRP) or grout (SRG) [4], have indicated that when epoxy resin is used the mechanical characteristics are significantly improved but the deformation capacity is smaller than in the case that grout is used.

Bond conditions for SRP and SRG laminates were examined in [5], the main test parameters being the anchorage length and the surface roughness. The main difference observed during those tests was with regard to the debonding level. When epoxy resin is used, surface concrete is detached, whereas when grout is used debonding takes place at the grout level. The effective anchorage length for SRP, FRP and SRG were found to be 127mm, 102mm, and 305mm, respectively. Results from bond tests were compared with predictions from nonlinear fracture mechanics models in [6]. It was found that debonding strength is influenced by the surficial tension strength, the number of SRP layers, and the anchorage width provided; the increase in strength is not directly proportional to the increase of the SRP anchorage width. Nonlinear fracture mechanics models specifically tailored to SRPs were found to predict more accurately the measured bond strength than models developed for CFRPs. Using the database compiled by Toutanji et al. [7], including 351 bond tests on polymers, 16 different analytical models for bond between concrete and SRP were evaluated. From this work, it was found that the analytical models proposed by Chen and Teng [8], Khalifa et al. [9], Yang et al. [10], and Yuan and Wu [11] provide good predictions of bond strength.

The first comparative tests on the use of SRP, SRG and CFRP for strengthening of R/C beams are reported in [12] and [13]. Consistently with the previously mentioned findings of tension tests, comparisons between SRP and SRG strengthened beams have shown that when a polymer (epoxy resin) is used as the matrix, the strength increase is higher than when a grout is used, but in the latter case the increase in deformation capacity is higher; strength increase varied between 40% and 70% [12]. In the case where CFRP was used, the increase in strength was 10% higher, while the deformation capacity was 24% lower than in the case that SRP or SRG was used [13]. The experimentally measured strengths were in good agreement with predictions based on (earlier versions of) the ACI 440.2R [14] Guidelines, when epoxy resin is used [15], [16]. An increase in the width of the SRP strips was found to increase the strength of the beams, but decrease their deformation capacity. The use of transverse, U shaped, SRP strips at the anchorage zone, was found to increase the strength as well as the deformation capacity [17]. The aforementioned results were confirmed in a series of tests on actual structures (buildings and bridges) in [3], [18], [19], [20], [21]. Also in [22] it was found that longitudinal SRP strips are better anchored when U-wraps at both ends of the specimens are used.

This paper reports results from the third (main) part of an experimental research programme focussing on the use of SRPs in strengthening of R/C beams and their relative merits with respect to the (so far) more widely used CFRPs. The first part [23] included tests for establishing the mechanical properties and stress – strain relationships for SRP and CFRP laminates. The second part focussed on the experimental determination of bond strength and deformation properties of SRP and CFRP strips externally bonded on the surface of concrete prisms. The main parameters studied were the anchorage length and width, the concrete grade, and the use of two types of SRP. Results from the first and second parts of this experimental programme are presented in [23], [24]. The present paper reports the design and fabrication of 13 full-scale specimens, the experimental set-up, and the results derived from these tests. The main parameters studied were

- the region of the beam (span or support of a continuous beam), which also affected the way loading was applied to the specimens; it is noted that, to the authors' best knowledge, no similar tests of specimens representing the support region of beams have been presented so far
- the different types of strengthening used (flexural or shear)
- the use of two types of SRPs for flexural strengthening
- the use of three types of reinforced polymers for shear strengthening,
- the use of either a continuous jacket or individual stirrups (strips) for shear strengthening
- the use of different anchorage length of polymer strips, and
- the use of smooth or ribbed reinforcement bars.

In addition to the test programme, the strength of the specimens was estimated analytically using equations based on principles of mechanics or of semi-empirical type, and the deformations recorded during the experiments.

2. Test programme

2.1 Specimen design

A total of 13 specimens, representing either the span or the support region of a continuous beam were tested. Specimens are separated into three groups. In the first group, the five specimens are designed, supported, and loaded in such a way as to simulate the response of the span of a continuous beam. In the second and third groups, consisting of four specimens each, the specimens simulate the response of the support region of a continuous beam. Fig. 1 shows the way the actual moment and shear force distribution in the continuous beam is approximated by the configuration of tested specimens representing the span and support regions.

The concrete used for the fabrication of the specimens was low strength, with a view to simulating the concrete grade typical in older concrete structures. The mean cylinder compressive

strength of concrete was 22.0 MPa, the mean cube strength was 26.4 MPa, and the tensile strength of concrete (estimated from the compressive strength) had a mean value of 2.4 MPa. The specimens were reinforced with smooth bars of diameter 8mm (Ø8) and 12mm (Ø12), and Ø12, Ø16 and Ø18 ribbed bars, whose stress – strain diagrams are given in Figures 2 and 3; details of the arrangement of steel reinforcement in the specimens are given in Figures 4 and 5 and discussed in subsequent sections.

Strengthening schemes

Six specimens were strengthened using two types of SRP strips, SRP 3X2 (cords made by twisting 5 individual wires together) and SRP 12X (cords made by twisting three 0.22mm wires and nine 0.20mm wires together). Four of them were strengthened in flexure and two in shear. Another three specimens were strengthened using CFRP strips, two of them in flexure using Sika Carbodur S512 strips and the third one in shear using Sika Wrap-300CZ strips. The materials used for strengthening the specimens are described in detail in [23], [24]. The remaining four specimens were tested unstrengthened, to serve as reference for comparisons with the strengthened specimens.

The nomenclature of the specimens was based on the beam region simulated by the specimen (span or support), the composite materials used for strengthening, and the expected failure mode. The first letter of the specimen name is "S" or "I" for "Span" and "Support" regions, respectively. The second part of the name is "V" for the unstrengthened specimen, "S3X2" or "S12X" for the specimens strengthened with different types of SRP, and "C" for the specimens strengthened with CFRP strips. The last part of the specimen name denotes the expected failure mode; it is "M" or "S" for flexural or shear type of failure, respectively, and "SM" for the case where the failure mode changes from shear to flexural after strengthening. Details of both the steel reinforcement of the specimens and the SRP or CFRP reinforcement used for strengthening are shown in Figs 4 and 5.

The design of the 13 specimens was carried out with a view to the intended failure mode. The three span specimens SCM, SS12XM and SS3X2M had conventional reinforcement (steel bars) identical to that of reference (or benchmark) specimen SVM. The expected mode of failure for all these specimens was flexural. In contrast with the actual response of an R/C beam subjected to uniformly distributed vertical loading, these specimens had a constant shear along the first and the last third of their length, due to the way the point loads were applied to the specimens (see bottom-left of Fig. 1). To compensate for this more unfavourable distribution, the specimens were reinforced by inclined Ø12 steel bars spaced at 25mm in the first and third part of their length (top of Fig. 4); it is worth pointing out that bent-up (inclined) bars are quite common in R/C members of older buildings, constructed prior to the adoption of modern seismic codes.

For the reference specimen SVS a shear failure mode was intended. The parameters studied in the corresponding group of specimens were the type of SRP, the use of CFRP, and the type of anchorage of the reinforced polymer strips; they were terminated either before or after the support

point of the specimen (see bottom of Fig. 4). The different anchorage schemes were explored in order to identify potential differences in the response of the specimens when the end region of the anchorage was free of tensile stresses or cracks, and check the deformation capacity of the reinforced polymer strip when the provided anchorage length is ample. It has to be clarified that the support points of the specimens do not correspond with actual supports (e.g. columns) of a continuous beam, as is clear from Figs. 1b, 1e; hence, the reinforced polymer reinforcement that extends beyond the specimen support is not really anchored beyond the actual support, but rather in a part of the beam beyond the contraflexure point.

The specimens ICM, IS12XM and IS3X2M represent the support region of the continuous beam and their steel reinforcement was identical to that of reference specimen IVM. Again, the shear force diagram in these specimens had a constant value in the left and right half of their length (bottom-right in Fig. 1), which is different from the actual shear distribution in the support region of a continuous beam subjected to uniform loading. For this reason the specimens were reinforced by inclined Ø12 steel bars spaced at 25mm. The same test parameters studied for the span specimens were also studied for the support specimen group. The span of these specimens was 2.2m (Fig. 5), while that of the span specimens was 3.2m (Fig. 4).

Specimens in the 'SM-group' (ICSM, IS12XSM and IS3X2SM) simulated the support of the continuous beam, and their steel reinforcement was identical to that of reference specimen IVS, for which a shear mode of failure was anticipated. The parameters studied for this last group were the use of two types of SRP, with two different configurations used for strengthening in shear, i.e. SRP continuous jacket (which is the most effective, but hardly feasible in actual T-beams, way of strengthening) or SRP stirrups (see bottom of Fig. 5), and the use of CFRP for one specimen (ICSM). It is worth noting here that fully closed stirrups (i.e. hoops) were used in the specimens, which is an easy solution for rectangular beams, but in practice the more common situation is that the R/C beam is integrally cast with a slab, in which case closing the stirrups is still feasible but rather cumbersome, since holes piercing the slab have to be drilled.

2.2 Experimental setup

The reaction frame of the Laboratory of Concrete and Masonry Structures of the Aristotle University, shown in Fig. 6, was used for the tests. A 1000kN double-acting hydraulic actuator was used for applying the vertical loading on the beam specimens, which, through the strong steel beam shown in Fig. 6 was finally applied as two point loads. For the specimens simulating the support region of a beam, the two point loads were applied over the middle 350mm of the specimens, i.e. very close to each other (simulating a column loading in an actual structure tested upside down), while in the span specimens they were applied at the third points ('four-point bending' test, see also Fig. 7). The specimens were supported at their ends on special rollers,

ensuring that the moment there had zero value. The loading was applied at a rate of 1mm/min and was controlled through a digital controller by comparing the measurements of the sensors of the actuator with the load command several times during each loading step.

Deflections and deformations of the specimen were measured by eight externally-mounted displacement sensors (LVDTs). The arrangement of the LVDTs mounted on a typical specimen and the corresponding nomenclature are shown in Fig. 7. The LVDT measurements and the recordings of the actuator's load-shell were used to draw the load vs. displacement or deformation diagrams shown in the remainder of the paper.

3.   Test results and failure modes of the specimens

3.1 Span Specimens

The reference specimen SVM showed a predominantly flexural response, as anticipated. Hairline flexural cracking initiated at a vertical deflection of 1.5mm (0.5‰ of its span) and an applied load of about 50kN (shear force of 25kN at each end). These cracks extended along the constant moment region (middle third of the specimen) and propagated only slightly with further loading up to a deflection of 9mm (load equal to 114kN); it was observed that their width was larger at the bottom of the beam, as expected. Subsequent to that level of loading only one crack, located close to mid-span, propagated further (top of Fig. 8) and inelastic deformation concentrated in this crack. As shown in Fig. 9, specimen SVM exhibited a stable post-yield resistance up to a rather large deflection (more than 30mm, i.e. about 1/100 of its span). The concentration of inelastic deformation at one crack only is clearly due to the poor bond conditions that characterise the smooth bars used as longitudinal reinforcement of the specimen. It is worth noting that the reinforcing bars of the specimen did not develop their full tensile strength, as loss of bond at the critical crack occurred at a stress lower than the tensile strength, as also verified by comparing the measured strength with the theoretical one calculated on the basis of the ultimate stress in the reinforcement.

The other reference specimen of the group, SVS, failed in shear, which was expected since it was over-reinforced in flexure with four large diameter (Ø18) ribbed bars (recall that SVM had only 4 Ø12 smooth bars at its bottom) but under-reinforced in shear. Hairline shear cracking initiated at a vertical deflection of 6.5mm and an applied load of about 180kN; this inclined cracking extended approximately from the loading points to the support points (bottom of Fig.8). The two shear cracks propagated with further loading up to the failure of the specimen. The strength of the specimen developed at a deflection of 12mm, corresponding to an applied load of 263kN and decreased after that point as shown in the force - deflection diagram of Fig. 9. As expected, this shear-critical specimen failed at a deflection (about 18mm) substantially lower than that developed by the flexural specimen. At the compression zone of specimen SVS, inelastic

deformations and spalling of concrete were observed above the shear cracks, accompanied by kinking-type buckling of steel bars; this was attributed to the combination of reduced (due to cracking) depth of the compression zone and the sparsely spaced stirrup reinforcement.

In the strengthened specimens SS3X2M, SS12XM, SCM, which had the same steel reinforcement as the reference flexural specimen SVM, hairline flexural cracking initiated at a deflection of about 5mm and extended along the middle third of the span as well as at the interior (i.e. towards mid-span) parts of the end thirds of the specimen (Fig. 8); cracks in specimen SCM (reinforced with CFRP strips) appeared later than in the SRP-reinforced specimens. Unlike the usual flexural cracks whose width increases from the neutral axis towards the bottom of the member, cracks in the strengthened specimen were practically closed (negligible width) at the bottom surface, attributed to the presence of the composite material that was bonded on this surface. Composites like SRP and CFRP have very high modulus of elasticity parallel to the direction of the fibres (measured values [23] were 67 and 78 GPa for the two SRP strips, and 160MPa for the CFRP strips), hence preventing crack opening in their vicinity. As the loading increased flexural cracks kept propagating but they remained almost closed at the bottom of the specimens; this is a pattern different from that found in ordinary R/C cracked members. Another notable feature was that flexural cracking was much better distributed in the strengthened specimens than in the reference one (SVM), wherein, as noted previously, only one of the initially formed cracks propagated significantly. The stiffness of the specimens started to degrade (see Fig. 9) at a deflection of about 10mm, when failure of the resin used for bonding the laminates on the concrete surface started (this was perceived during the test by sharp noises, characteristic of debonding). As noted from the slopes of the diagrams in Fig. 9, the reduced stiffness remained almost constant up to the failure (due to debonding) of the SRP or FRP strips. Subsequent to debonding, the strength of the specimens dropped to a level slightly lower than that of the strength of the reference specimen, indicating that, apparently due to the different cracking pattern, steel bars did not develop (at that stage) the stress developed in the bars of the unstrengthened beam. By further increasing the applied displacement, the strength of the specimen increased up to a value close to the strength level of the initial specimen, while all inelastic deformation concentrated in the longitudinal (smooth) reinforcement at one main flexural crack. After that point, the response of the specimen was almost identical with the one of the unstrengthened specimen.

As far as the efficiency of the strengthening scheme is concerned, it was found that the increase in strength was about 90%, which is quite satisfactory. While for all strengthened specimens failure initiated with debonding at a flexural crack, those strengthened with SRP strips have developed slightly larger ultimate deflections. The specimen strengthened with SRP type 3X2 exhibited an ultimate deflection 4% higher than that of the CFRP-strengthened specimen; the increase was even larger (17%) when SRP type 12X was used. Fig. 10 shows load vs. elongation of the bottom side

(at midspan) of the span specimens (recordings from HMT sensor in Fig. 7). The different types of failure are clearly noted in the figure, since the shear-dominated specimen SVS displayed a very small amount of elongation at the bottom of its mid-span, quite distinct from the large elongations (characteristic of flexural deformations) developed by the other specimens. As is also clear from Fig. 8 (bottom) the largest part of the deflection of SVS was due to the rotation caused by the opening of shear cracks (in particular the left one in the figure). It is also noted that in specimen SS12XM debonding of the SRP strip took place for a larger elongation than in the specimens where a longer anchorage length was used (bottom of Fig. 4); this hints to the fact that debonding started at a flexural crack away from the anchorage zone, hence the anchorage length had no noticeable effect on the ultimate deformation.

3.2 Support specimens strengthened in flexure

The reference specimen IVM has shown, as expected, a predominantly flexural behaviour. Hairline flexural cracking in the maximum moment region (where the loading was applied, see Fig. 1) initiated at a vertical deflection of 1.2mm and an applied load of about 58kN (shear force of 29kN at each end). Similarly to the case of specimen SVM, hairline flexural cracking propagated only slightly with further loading and inelastic deformation concentrated in one major crack located in the middle of the specimen, as shown at the top of Fig. 11. As discussed in the previous section this is due to the use of smooth longitudinal reinforcement in the specimen. Up to the application of a deflection of about 5mm the load resisted by the specimen kept increasing (up to about 170kN). As shown in Fig. 12, after that stage the resistance of the specimen practically stabilised up to an applied deflection of 20mm (1% the specimen length) wherein the test was terminated. No visible shear cracks developed in this specimen and measured shear deformations (LVDTs DL, DR in Fig. 7) were negligible; this was not surprising since the specimen was over-designed against shear, as discussed in previous sections.

The strengthened specimens of this group have shown a response similar to that of the corresponding specimens of the first group (span specimens), there were, nevertheless, some differences that are worth mentioning, for instance, as shown in Fig. 11, flexural cracking developed over a shorter length (which is consistent with the different bending moment distribution in the span and support specimens).

As far as the efficiency of the strengthening scheme is concerned, the relative strength increase in the support specimens was lower than in the span specimens. With regard to the two types of reinforced polymer strips used (SRP and CFRP), the tests have shown that the SRPs were equally effective as the CFRP used for specimen ICM. In addition to strength, another important parameter studied was the way the reinforced polymer strips were anchored at the end of the specimens (see top of Fig. 5). The longer anchorage length, extending into the stress-free region beyond the roller

supports (which did not make contact with the strips) used in specimens ICM and IS12XM was found to have a rather significant effect on the strength increase or the deformation capacity of the specimens. In Fig. 13, where the load vs. elongation of the bottom side diagrams are shown, it is clear that specimen IS3X2M where the anchorage terminated before the support points strength dropped more abruptly and for a smaller deformation than for the other two specimens that had longer anchorage lengths. These observations hint to the fact that in the support specimens (which are shorter than the span ones) the anchorage type has a more noticeable influence on strength and deformation capacity, apparently because debonding failure started at the end of the strips, rather than at a flexural crack in the maximum moment region (as in the span specimens).

3.3 Support specimens strengthened in shear

The reference specimen (IVS) of this third group has shown, a shear-dominated behaviour, as expected, since the specimen was heavily reinforced in flexure (4Ø16 ribbed bars), and lightly reinforced in shear (see bottom part of Fig. 5). Hairline shear cracking appeared in the end regions of the specimen for a mid-span deflection of about 2mm, corresponding to a load of 125kN (shear of 62.5 kN at each end). The width of these shear cracks increased with further applied deflection, up to failure, which occurred at the right end as shown in Fig. 14. Referring to the load vs. deflection diagram of Fig. 15, it is seen that the peak strength of the specimen (224.8kN, i.e. a shear of 112.4kN) developed for a mid-span deflection of 6.6 mm and the resistance degraded thereafter, which is typical of shear failures.

In contrast with the reference specimen IVS, specimens IS3X2SM, IS12XSM and ICSM, which had the same longitudinal reinforcement as IVS but were strengthened against shear as shown in Fig. 5 (and described in section 2.1) have shown a predominantly flexural response. At the initial stages of loading no visible damage appeared, especially in the two specimens that were strengthened with a composite jacket. Flexural cracks that appeared later than in the reference specimen could be detected between the cords of the SRP material (recall that the SRP was placed with its fibres parallel to the flexural cracks), and, as shown in Fig. 14, were concentrated in the central region of the specimen, as expected (maximum moment region). In the specimen IS12XS-M that was reinforced with stirrup-type SRP reinforcement, flexural cracks appeared for a 5.8 mm deflection. At a later stage (30mm deflection) shear-flexural cracks formed, whose inclination increased with their distance from the middle of the specimen, as shown in Fig. 14, and their width was smaller than that of the main flexural cracks. The predominantly flexural response of all strengthened specimens can be also seen from the load-deflection diagrams of Fig. 15, where it is clear that after the initial yielding of the longitudinal reinforcement, the strength of the specimens kept increasing (slightly), clearly due to the strain-hardening of the steel bars. At the final stage of the response signs of crushing of the compression zone were also detected, while there was no

indication of debonding of the polymer strips. Consistently with the previous remarks regarding the predominance of shear or flexure, the strengthened specimens developed an ultimate deflection of at least 35mm (Fig. 15), whereas the reference specimen IVS failed at a deflection of only 17mm.

Since shear response was a key parameter in this group, it is important to focus on measured shear deformations. From the load vs. diagonal elongation diagrams (LVDT 'DR' in Fig. 7) given in Fig. 16, the large difference between the shear-critical specimen IVS and the strengthened specimens can be seen; the diagonal deformation is 8mm in the former and only 3mm in the latter, despite the fact that the shear developed in the strengthened specimens was about 100% higher than in IVS.

Finally, with respect to the effectiveness of the various strengthening schemes, it was noted that the two schemes involving SRP (in the form of a single-layer jacket in IS3X2SM, and with half the SRP quantity, in the form of 50mm-wide closed stirrups, in IS12XSM) were equally effective as the CFRP strengthening scheme (jacket) used in specimen ICSM.

4. Analytical prediction of measured flexural and shear strength

An attempt was made to predict analytically the flexural and shear strengths of the specimens, using measured deformation quantities. These quantities were introduced into fundamental equations of mechanics in the case of flexure, and into the Eurocode 8-3 [25] semi-empirical equations in the case of shear, as discussed in the following.

For the flexural strength of the unstrengthened (reference) specimens the following relationship was used [26]:

$$M_R = A_{s1} \cdot \sigma_{s\max} \cdot (d - \delta_G \cdot x) + A_{s2} \cdot E_s \cdot \varepsilon_{s2} \cdot (\delta_G \cdot x - d_2) \tag{1}$$

where: A_{s1} = area of tension reinforcement (steel)

A_{s2} = area of compression reinforcement (steel)

σ_{smax} = max stress in steel reinforcement

E_s = modulus of elasticity of steel

ε_{s2} = compression steel strain

ε_s = tension steel strain

d = effective depth of the specimen

h = total depth of the specimen

d_2 = distance from the centroid of compression steel to the outer compression fibre

x = depth of the compression zone (neutral axis depth)

δ_G = coefficient for the location of the resultant of compression forces in the section:

$$\delta_G = \begin{cases} \dfrac{8 - 1000 \cdot \varepsilon_c}{4 \cdot (6 - 1000 \cdot \varepsilon_c)} & for \ \varepsilon_c \leq 0.002 \\[2em] \dfrac{1000 \cdot \varepsilon_c \cdot (3000 \cdot \varepsilon_c - 4) + 2}{2000 \cdot \varepsilon_c \cdot (3000 \cdot \varepsilon_c - 2)} & for \quad 0.002 \leq \varepsilon_c \leq 0.0035 \end{cases} \tag{2}$$

The neutral axis depth can be expressed in terms of the concrete and steel strains from the linear strain profile assumption (Bernoulli):

$$\frac{\varepsilon_c}{x} = \frac{\varepsilon_s}{h - x} \tag{3}$$

As noted in the previous section, the tests have shown that the smooth steel bars used as longitudinal tension reinforcement did not reach their ultimate strain. In all cases, for a steel strain value in-between the yield and the ultimate strain, bond failure started and subsequent (critical) crack opening took place without noticeable increase in steel strain. Based on measured loading (and hence, bending moment) the steel stress at which bond failure started was 412MPa, which corresponds to a strain of 6.5% (Fig. 2); therefore, σ_{smax} =412MPa was introduced in equation (1). The concrete and steel strains required in equation (3) were calculated from the recordings of the horizontal LVDTs mounted on the top and bottom of the specimens (HMC, HMT in Fig. 7).

Using the aforementioned measured quantities the moment capacity of the unstrengthened specimens was calculated from equation (1) and the corresponding shear was calculated from equilibrium. For the support specimen IVM the flexural capacity was found to be 78.25kNm, hence the shear is 78.25/0.925=84.6 kN and the corresponding (total) loading P=2×84.6=169.2 kN, quite close to the measured value (172.9 kN). This value was taken as the basis for calculating the strength of all strengthened specimens in the 'support group'.

As noted in the previous section, the strength immediately after debonding of the strengthened specimens (V_{crit}) was slightly lower than the final strength (V_{fin}) developed by each specimen when further loading (displacement) was applied, see Table 1 and Fig. 17. The value of V_{crit} (and hence of M_{crit}) was estimated analytically from equations (1) to (3) by introducing a steel stress for the longitudinal reinforcement equal to the yield strength of the bars, i.e. σ_{smax}=f$_y$=346.9 MPa. This apparently low stress of the reinforcement is deemed justified in the light of the following observations made during the tests:

    i. Debonding of the reinforced polymer strips took place for generally low deflections

    ii. Just prior to debonding, flexural cracks were almost closed, indicating the absence of post-yield deformation of the steel bars.

    iii. In the strengthened specimens several, almost uniformly distributed, cracks formed which hints to the fact that at the debonding stage tensile deformations were distributed rather uniformly among the cracks.

The strength increase in the specimens due to the presence of the externally bonded SRP or FRP strips can be estimated from the relationship [26]:

$$M_{R,f} = A_f \cdot E_f \cdot \varepsilon_f \cdot \left(h - \delta_G \cdot x\right) \tag{4}$$

where the various symbols have the same meaning as in equation (1), while the subscript 'f' refers to the reinforced polymer strip. Introducing in (4) the material and geometric properties of the strips, and the values recorded by the pertinent LVDTs, the additional flexural strength $M_{R,f}$ is estimated and the corresponding $V_{R,f}$ is found from equilibrium.

It is known from the literature, e.g. Teng et al. [27], that in regions of beams where flexural cracking exists the effective strain (ε_f) of the polymer, and hence the force that causes debonding, are increased, and the additional strength $V_{R,f}$ should be increased by 30%; therefore, the total strength at debonding is $V_{deb} = V_{crit} + 1.30 \cdot V_{R,f}$. In the present study the average increase for the flexurally-strengthened support specimens was found to be 14%, i.e.

$$\frac{\sum\left[\left(V_{deb,i,EXP} - V_{crit}\right)/V_{R,f\_i}\right]}{\sum i} = 1.14 \tag{Σi=3}$$

therefore, the total strength at debonding was calculated from:

$$V_{deb} = V_{crit} + 1.14 \cdot V_{R,f} \tag{5}$$

For the flexurally-strengthened span specimens the same approach was used but a different average increase in strength was found in the tests and used for calculating the total strength. More specifically, the strength of the reference specimen SVM was found (from the corresponding moment capacity) to be 56.6 kN (total load P= 113.2 kN), slightly lower than the measured value (P=117.6 kN). The average increase in the part of strength due to the reinforced polymer strips was quite higher than that for the support specimens (40%), hence the total strength was estimated from:

$$V_{deb} = V_{crit} + 1.40 \cdot V_{R,f} \tag{6}$$

It is noted that the ratio of increase in $V_{R,f}$ in equations (5) and (6) is 0.40/0.14=2.86 is the same as the ratio of constant moment regions (or the distance between the applied concentrated loads, see Figs. 4, 5, 7) in the span and support specimens, i.e. 1.00/0.35=2.86. This hints to the conclusion that the factor to be applied to $V_{R,f}$ in flexurally strengthened beams is 1+0.4ℓ_{CBM} where ℓ_{CBM} is the length (in m) of the constant bending moment region.

Three different procedures were used to estimate the shear strength of the support specimens, two based on the European practice (Eurocodes) and one on the North-American practice (ACI codes), as presented in the following.

Unlike most other codes, Eurocode 2 [28] adopts the variable angle truss model without a 'concrete contribution'; in this case a reasonable value has to be used for the angle (θ) of inclination of the compression struts, to be introduced in

$$V_{RC} = \frac{A_{sw}}{s} \cdot z \cdot \sigma_{sw} \cdot \cot\theta \qquad (7)$$

where A_{sw} is the area of shear reinforcement (stirrups or inclined bars) spaced at a distance s, σ_{sw} the stress developed by this reinforcement (usually taken as the yield strength), and $z \approx 0.9 \cdot d$ is the internal lever arm of the section. The angle of the inclined struts (which according to Eurocode 2 can be taken between 22º and 45º) was taken equal to 31º and 28º for specimens IVS and SVS, respectively, on the basis of the test observations (average inclination of the critical shear crack); the yield strength of the shear reinforcement was 311 MPa (Fig. 2). Introducing the previous values in equation (7) the shear strength of IVS and SVS was found to be 85.5 and 96.7 kN, respectively, and the corresponding applied loads 171.0 and 193.4 kN, which are lower than the measured values of 224.8 and 263.6 kN, respectively. Since ignoring the concrete contribution (V_c) is not only a controversial choice but also different from what the previous ('Prestandard') version of the Code adopted, an alternative estimation ('old EC2') of shear strength was also made, wherein a V_c term was added to the term corresponding to the shear reinforcement, but a 45º angle of shear cracks was used (i.e. equation 7 with $\cot\theta=1$) as required by 'old EC2' and other codes (like ACI).

In the ACI approach a concrete contribution ($V_c=017\sqrt{f_c}\cdot b_w \cdot d$) is added to the truss contribution of equation (7), wherein $\theta=45$º is assumed. The resulting shear strength is 112.4 for both specimens (IVS and SVS), since the same angle θ is used, corresponding to a total load of 224.9 kN, which is very close to the measured value for IVS (and lower than that for SVS).

Although the shear- strengthened support specimens failed in flexure, it was deemed interesting to estimate their shear strength and check that this was, indeed, higher than the actually recorded strength. The additional shear strength V_f provided by the SRP or CFRP strips, having a width w_f and thickness t_f, was estimated using the following relationship (adopted by Eurocode 8 – Part 3 [25])

$$V_{Rd,f} = 0.9 \cdot d \cdot f_{fdd,e,W} \cdot 2 \cdot t_f \cdot \left(\frac{w_f}{s_f}\right)^2 \cdot (\cot\theta + \cot\beta) \cdot \sin\beta \qquad (8)$$

where $\beta=90$º when the fibre direction in the FRP strip is perpendicular to the axis of the member (as here), and $f_{fdd,e,W}$ is the design effective debonding strength, which depends on the strengthening configuration; for fully wrapped FRP (or SRP, in the absence of more specific information), this strength is taken equal to

$$f_{fdd} \cdot \left[1 - k\frac{L_e \cdot \sin\beta}{2z}\right] + \frac{1}{2}\left(f_{fu,W}(R) - f_{fdd}\right) \cdot \left[1 - \frac{L_e \cdot \sin\beta}{z}\right] \tag{9}$$

where L_e is the effective bond length, $f_{fu,W}$ is the ultimate strength of the FRP strip or sheet, f_{fdd} is the design debonding strength, and $k = (1 - 2/\pi)$. The spacing s_f of the FRP strips should be taken equal to w_f for sheets. Appropriate values for all other quantities in equations (8) and (9) are given in Appendix A of EC8-3 and will not be reproduced here for economy of space.

The ACI Guide for the design of FRP-strengthened R/C members [14] adopts the following equation for the additional shear strength V_f provided by FRP strips

$$V_f = \frac{A_{fv} \cdot f_{fe} \cdot (\sin a + \cos a) \cdot d_{fv}}{s_f} \tag{10}$$

where $A_{fv} = 2nt_f w_f$, d_{fv} is the effective depth of FRP shear reinforcement, the effective stress $f_{fe} = \varepsilon_e E_f$ and the effective strain $\varepsilon_{fe} = 0.004 \le 0.75\varepsilon_{fu}$ for fully wrapped members; the limiting strain of 0.004 is usually the critical one.

Assuming $\theta=45°$ and applying equations (8) and (9) the shear strengths of the strengthened support specimens were estimated to be 120.5, 356.25 and 486.20 kN, for IS12XSM, IS3X2SM, and ICSM, respectively, corresponding to total strengths. Similar strength values were estimated using the ACI equation (10), i.e. 129.2, 300.8, and 397.3 (the value for IS3X2SM is rather lower than that predicted by the EC8-3 equation).

It is clear that for the two fully-wrapped specimens IS3X2SM, and ICSM the total shear strengths are far in excess of the measured peak values (summarised in Table 1) which are obviously flexure-controlled. For the specimen (IS12XSM) with SRP strips (Fig. 5), the estimated total shear strength varies from 206.0 to 232.9kN, depending on whether the Eurocode or the ACI procedure is used for estimating the strength of the unstrengthened specimen. Hence the corresponding loads are 412.0 and 465.8 kN, which exceed the measured value of ultimate load (402.60 kN), but by a small margin only, indicating that this beam failed in a mixed flexure-shear mode, an observation which generally agrees with the observed behaviour (Fig. 14).

5. Conclusions

The present study has shown that flexural strengthening of R/C beams with SRP strips can lead to substantial increases in strength; this increase was about 90% for span specimens and about 80% for support specimens. Moreover, higher deformation capacity (up to 17%) was found for the specimens strengthened with SRP, compared to the specimens strengthened with CFRP. Given that

SRP materials are less expensive than CFRP, it is clear that they represent an attractive alternative for strengthening of R/C members.

The present study included both span and support specimens, permitting comparisons regarding the efficiency of strengthening techniques (with SRP and CFRP strips) in each case. Flexural failure of support specimens took place for a deformation about 50% lower than that of span specimens. This shows that flexural strengthening of the support regions of beams is not necessarily beneficial for their inelastic response since, despite the increased strength, their deformability is adversely affected, due to debonding of the reinforced polymer at a relatively low deformation. This aspect is particularly relevant in the case of seismic loading, which was not the focus of the present study.

The increase in the effective strain of the fibre-reinforced polymer in regions of beams where flexural cracking exists, which is known from previous studies, was found here to depend on the length of the constant bending moment region; a good estimate of this increase (and hence of the force at debonding) can be obtained from $0.4\ell_{CBM}$ where ℓ_{CBM} (in m) is the aforementioned length.

Alternative detailings of the end anchorage of strengthening strips were tested, including a new one wherein the strips were anchored beyond the end supports of the specimen. In the case of span specimens no visible effect of the anchorage type was found, attributed to the fact that strength was governed by debonding at an intermediate crack rather than by cover delamination at the tip of the anchorage. On the contrary, in the case of support specimens, the improved anchorage scheme led to 33% increase in the deformation of the tension side and a subsequent increase in deflection. This suggests that improving anchorage conditions is more of an issue in support regions of beams, but clearly more work is required in this direction.

The present study focused on existing structures representative of prevailing practice 40-50 years ago, hence smooth reinforcement bars were used in most specimens. In these specimens it was found that subsequent to yielding of longitudinal rebars and/or debonding of the reinforced polymer strip the load-deflection curve for the beam becomes rather flat (instead of ascending), indicating that in members with smooth bars hardening of steel does not affect the response which is governed by bond conditions of the smooth bars.

Strengthening of beams against shear (by vertical hoops or continuous full wrapping of the member) was found to lead to substantial increases in shear strength. Notably, whereas the reference (unstrengthened) specimen failed in shear, all strengthened specimens in the same series failed in a flexural mode. The successful shear strengthening led to increases in strength of about 90% and in deformability of about 100%. The flexural strength of specimens strengthened in shear was found to be higher than that of the theoretical strength of the unstrengthened specimen (i.e. that due to steel reinforcement alone). As expected, this increase was higher (12%) in the case of fully wrapped members and lower (5%) in the case of strengthening with SRP strips.

Finally, comparisons of analytically predicted strengths with experimentally measured values has shown that the equations developed for FRP-strengthened beams can also be used for SRP-strengthened members.

References

[1] Matteson, R. and Crane, R. Flexural Testing of Steel Wire Composite Beams Made with Hardwire[TM] Unidirectional Tape. Naval Surface Warfare Center Carderock Division, Survivability, Structures and Materials Department, Technical Report, 2003.

[2] Kim, J.Y., Fam, A., Kong, A. and El-Hacha, R. Flexural Strengthening of RC Beams Using Steel Reinforced Polymer (SRP) Composites. In: 7th Int. Symp. FRP Reinforcement for Concrete Structures, SP-230, ACI Vol. 1, Farmington Hills, USA, 2005. Paper # 93.

[3] Huang, X., Birman, V., Nanni, A. and Tunis, G. Properties and Potential for Application of Steel Reinforced Polymer (SRP) and Steel Reinforced Grout (SRG) Composites. Compos Part B: Eng 2005; 36(1):73-82.

[4] Barton, B.L., Wobbe, E., Dharani, L.R., Silva, P.F., Birman V., Nanni, A., Alkhrdaji, T., Thomas, J. and Tunis, T. Characterization of RC Beams Strengthened by Steel Reinforced Polymer and Grout (SRP and SRG) Composites. Materials Science and Engineering A 2005; 412:129.

[5] Matana, M., Nanni, A., Dharani, L., Silva, P. and Tunis, G. Bond Performance of Steel Reinforced Polymer and Steel Reinforced Grout. In: Proceedings of International Symposium on Bond Behaviour of FRP in Structures, BBFS 2005. Paper # 101.

[6] Figeys, W., Schueremans, L., Brosens, K. and Van Gemert, D. Strengthening of Concrete Structures using Steel Wire Reinforcement Polymer. In: Proceedings of 7th Int. Symp. FRP Reinforcement for Concrete Structures, SP-230, ACI Vol. 1, Farmington Hills, USA 2005, Paper # 43.

[7] Toutanji, H., Saxena, P., Zao, L. and Ooi, T. Prediction of Interfacial Bond Failure of FRP-Concrete Surface. J Compos Construct 2007;11(4):427-436.

[8] Chen, J., and Teng, J. Anchorage Strength Models for FRP and Steel Plates Bonded to Concrete. J Structural Engineering 2001; 127(7):784-791.

[9] Khalifa, A.,Gold, W. J., Nanni, A., and Aziz, A. Contribution of Externally Bonded FRP to Shear Capacity of RC Flexural Members. J Compos Construct 1998; 2(4):195-202.

[10] Yang, Y. X.,Yue, Q. R., and Hu, Y. C. Experimental study on bond performance between carbon fibre sheets and concrete. J Building Structures 2001; 22(3):36-42.

[11] Yuan, H., and Wu, Z. Interfacial fracture theory in structures strengthened with composite of continuous fibre. In: Proceedings of Symposium of China and Japan: Science and Technology of the 21st Century, Tokyo, 1999.

[12] Wobbe, E., Silva, P.F., Barton, B.L., Dharani, L.R., Birman, V., Nanni, A., Alkhrdaji, T., Thomas, J. and Tunis, T. Flexural Capacity of RC Beams Externally Bonded with SRP and SRG. In: Proceedings of Society for the Advancement of Material and Process Engineering, symposium, Long Beach, Ca, USA, 2004.

[13] Prota, A., Manfredi, G., Nanni, A., Cosenza, E. and Pecce, M. Flexural Strengthening of RC Beams using Emerging Materials: Ultimate Behavior. In: Proceedings of 2nd Int. Conf. on FRP Composites in Civil Engineering, CICE 2004, Adelaide, Australia, 2004.

[14] ACI Committee 440 "*Guide for the Design and Construction of Externally Bonded FRP Systems for Strengthening Concrete Stuctures*" (ACI 440.2R-08), Farmington Hills, Michigan, USA, 2008.

[15] Pecce, M., Ceroni, F., Prota, A. and Manfredi, G. Response Prediction of RC Beams Externally Bonded with Steel Reinforced Polymers. J Compos Construct 2006;10(3):195-203.

[16] Prota, A., Tan Yong, K., Nanni, A., Pecce, M. and Manfredi, G. Performance of Shallow RC Beams with Externally Bonded Steel-Reinforced Polymer. ACI Struct J 2006;103(2):163-170.

[17] Kim, J.Y., Fam, A., Kong, A. and El-Hacha, R. Flexural Strengthening of RC Beams Using Steel Reinforced Polymer (SRP) Composites. In: Proceeding of 7th Int. Symp. FRP Reinforcement for Concrete Structures, SP-230, ACI Vol. 1, Farmington Hills, USA 2005, Paper # 93.

[18] Casadei, P., Nanni, A., Alkhrdaji, T. and Thomas, J. Performance of Double-T Prestressed Concrete Beams Strengthened with Steel Reinforced Polymer. In: Proceedings of 7th Int. Symp. FRP Reinforcement for Concrete Structures, SP-230, ACI Vol. 1, Farmington Hills, USA 2005, Paper # 44.

[19] Casadei, P., Nanni, T., Alkhrdaji, T. and Thomas, J. Performance of Double-T Prestressed Concrete Beams Strengthened with Steel Reinforced Polymer. Advances in Structural Engineering - International Journal 2005;8(4):427-442.

[20] Casadei, P., Nanni, A. and Alkhrdaji, T. Steel Reinforced Polymer: an Innovative and Promising Material for Strengthening the Infrastractures. Concrete Engineering International, UK 2005;9(1):54-63.

[21] Lopez, A., Galati, N., Alkhrdaji, T. and Nanni, A. Strengthening of a Reinforced Concrete Bridge with Externally Bonded Steel Reinforced Polymer (SRP). Compos Part B: Eng 2007; 38(4): 429-436.

[22] Saber, N., Hassan, T., Abdel-Fayad, A. S. and Gith, H. Flexural behavior of concrete beams strengthened with steel reinforced polymers. In: Proceedings of 4th Int. Conf. on FRP Composites in Civil Engineering, CICE 2008, Zurich, Switzerland.

[23] Mitolidis, G.J., Salonikios, T.N., and Kappos, A.J. Mechanical and Bond Characteristics of SRP and CFRP Reinforcement – A Comparative Research. The Open Construction and Building Technology Journal, 2008; 2:207-216.

[24] Mitolidis, G., Salonikios, T. and Kappos, A. Bond Tests of SRP and CFRP – Strengthened Concrete Prisms. In: Proceedings of 4th Int. Conference on FRP Composites in Civil Engineering (CICE2008), Zurich, Switzerland, Paper # E111.

[25] CEN (Comité Européen de Normalisation). Eurocode 8: Design of Structures for Earthquake Resistance - Part 3: Assessment and retrofitting of buildings (EN 1998-3:2005). Brussels, March 2005.

[26] *fib*. Externally bonded FRP reinforcement for RC structures. *fib* Bull. 14, Lausanne, 2001.

[27] Teng, J.G., Chen, J.F., Smith, S.T. and Lam, L. *FRP Strengthened RC Structures*. John Wiley & Sons Ltd,Chichester, England, 2002, 245pp.

[28] CEN Techn. Comm. 250 "Eurocode 2: Design of Concrete Structures - Part 1-1: General rules and rules for buildings (EN 1992-1-1)", CEN, Brussels, 2004.

Table 1. Calculated versus experimentally measured strengths of the specimens.

	Calculated Strength					Experimental strength					$P_{max,an}$ / $P_{max,exp}$
	P_{deb}	P_{crit}	P_{fin}	P_y	P_u	P_{deb}	P_{crit}	P_{fin}	P_y	P_u	
	kN	kN	kN	kN	kN	kN	kN	kN	kN	kN	-
Specimen											
SVS	-	-	-	-	193.3/240.7/224.9	-	-	-	-	263.60	0.85
SVM	-	-	113.24	-	-	-	-	117.60	-	-	0.96
SS3X2M	231.01	95.56	113.24	-	-	225.60	86.60	108.40	-	-	1.02
SS12XM	216.45	95.56	113.24	-	-	218.00	83.60	102.80	-	-	0.99
SCM	203.36	95.56	113.24	-	-	224.80	96.40	105.20	-	-	0.91
IVM	-	-	169.19	-	-	-	-	172.97	-	-	0.98
IS3X2M	278.45	142.57	169.19	-	-	277.20	159.20	164.40	-	-	1.00
IS12XM	294.60	142.57	169.19	-	-	302.80	146.40	160.00	-	-	0.97
ICM	299.27	142.57	169.19	-	-	289.20	148.00	160.80	-	-	1.03
IVS	-	-	-	-	171.1/231.3/224.9	-	-	-	-	224.80	1.00
IS3X2SM	-	-	-	313.02	392.11	-	-	-	397.20	430.80	0.91
IS12XSM	-	-	-	314.36	383.44	-	-	-	364.40	402.60	0.95
ICSM	-	-	-	314.51	385.23	-	-	-	382.80	438.00	0.88

Note: P_{deb}, P_{crit}, P_{fin}, and P_u are defined in Fig. 17. The three P_u values (6th column) are based on EC2, old EC2, and ACI-318, respectively.
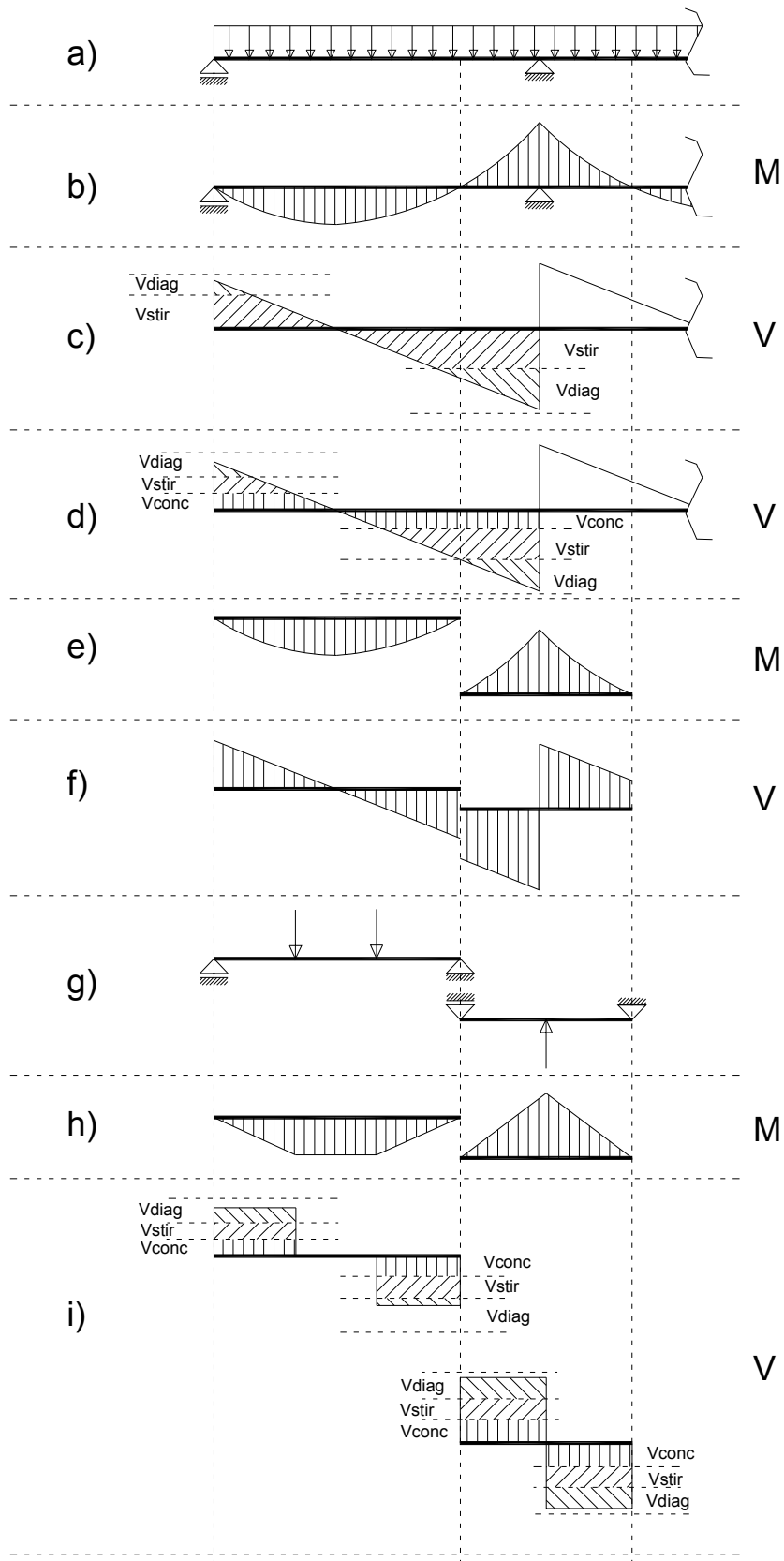
Figure 1. Moment and shear force distribution in the actual continuous beam (upper part) and in the specimens tested, and shear design procedure used (Vconc, Vstir, Vdiag, refer to the shear carried by concrete, stirrups, and bent-up bars, respectively).
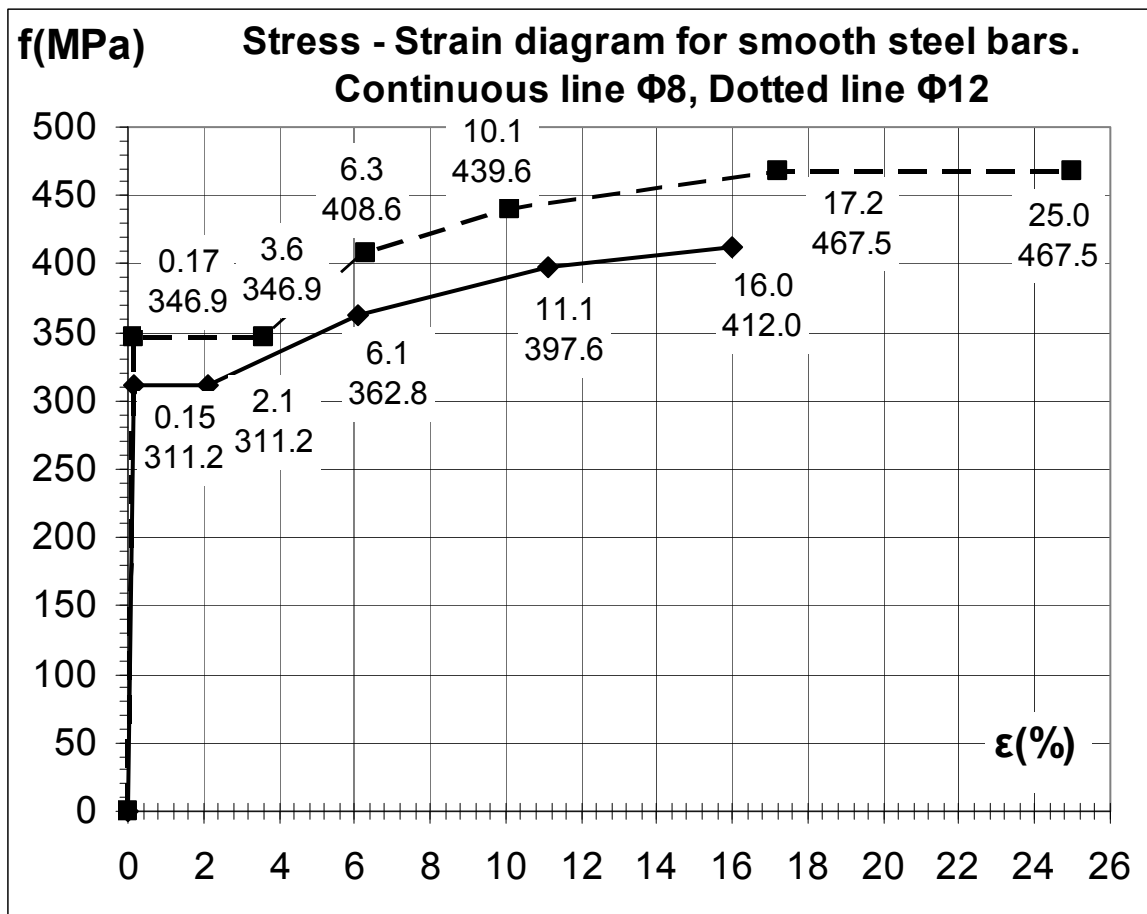
Figure 2. Stress – strain diagrams for Ø8 and Ø12 smooth reinforcement bars.
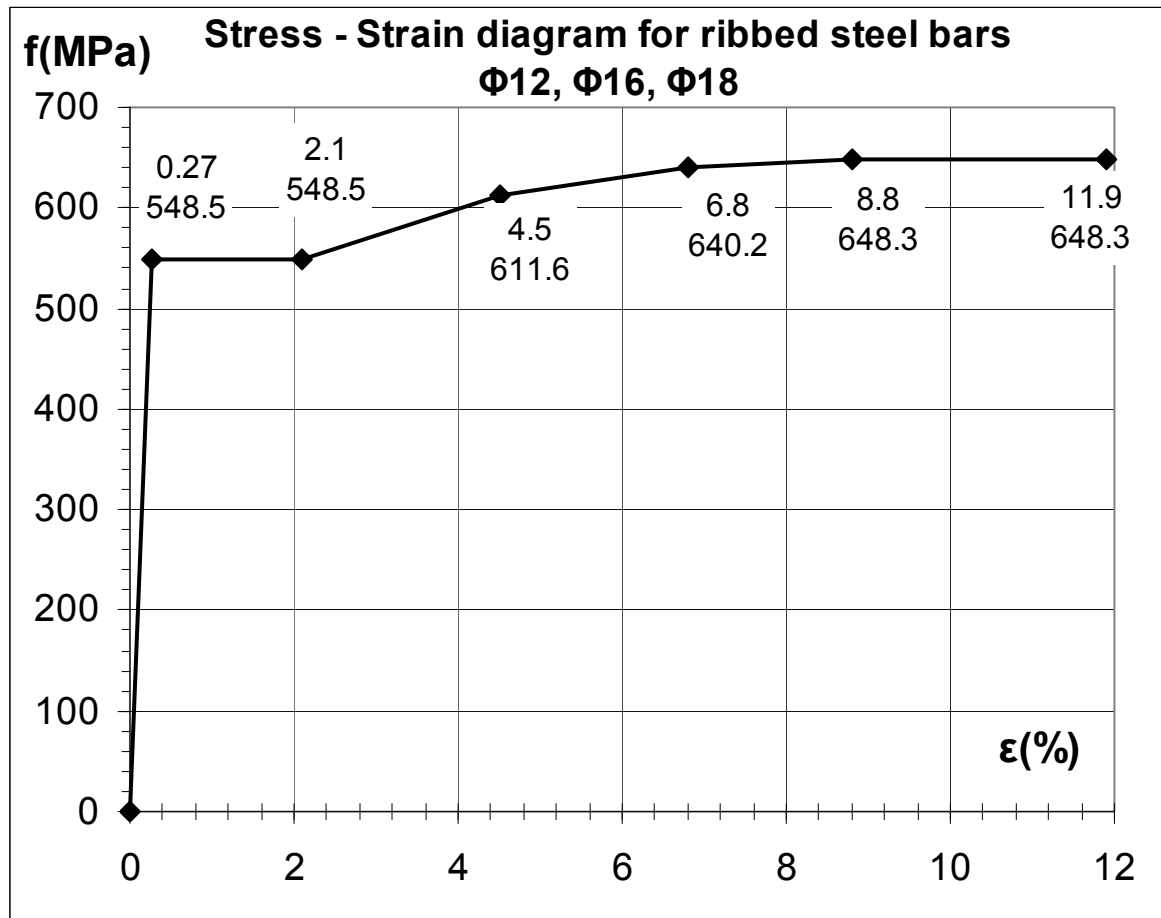
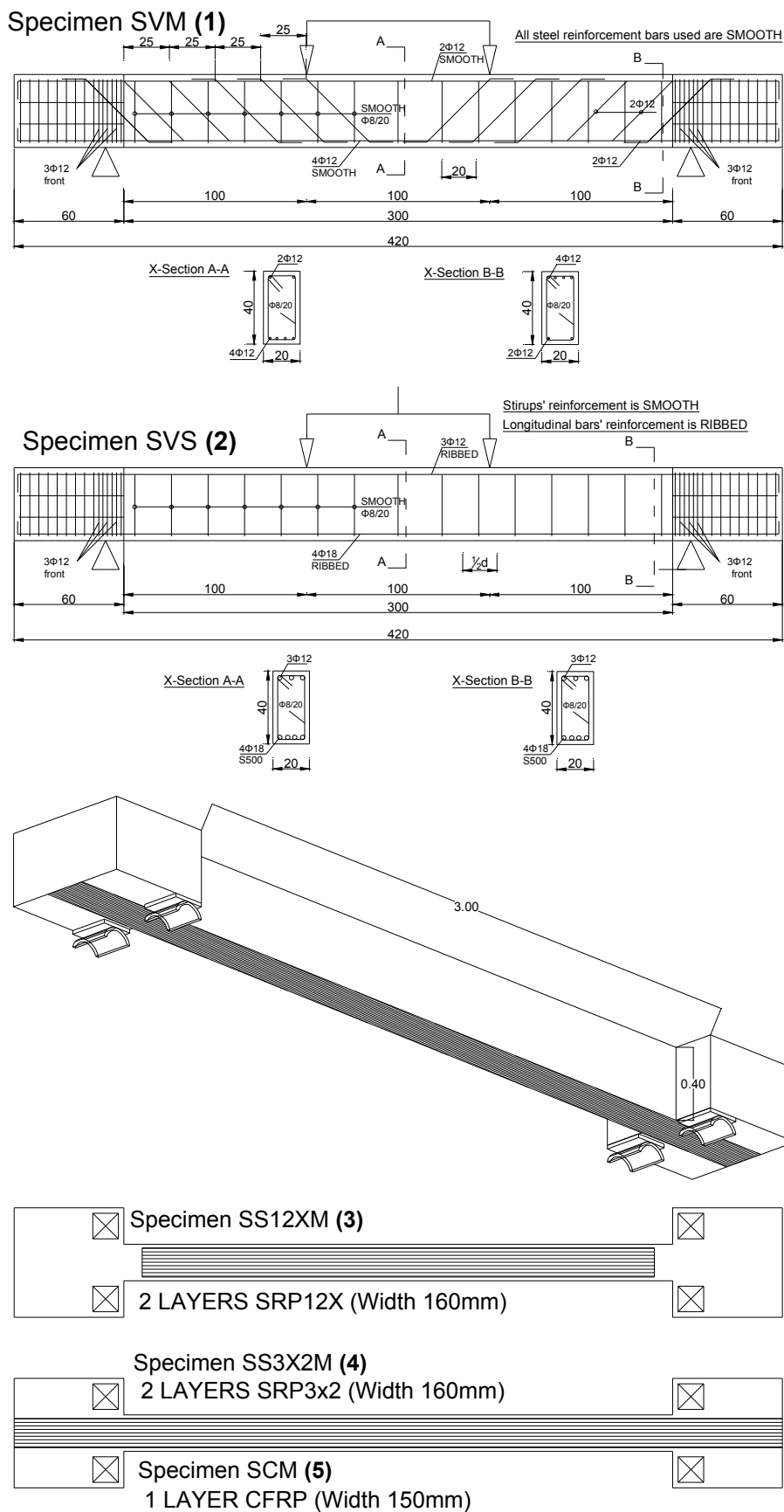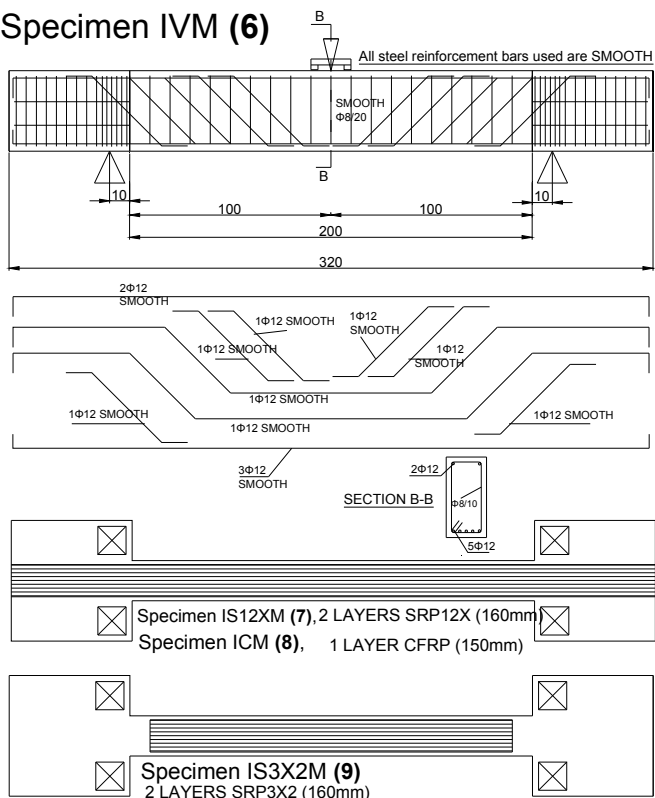Figure 3. Stress – strain diagrams for Ø12, Ø16 and Ø18 ribbed reinforcement bars.

Figure 4. Details of the specimens that represent the span of a continuous beam.

Specimen IVM **(6)**

B

All steel reinforcement bars used are SMOOTH

SMOOTH
Φ8/20

B

10 | 100 | 100 | 10

200

320

2Φ12
SMOOTH

1Φ12 SMOOTH

1Φ12
SMOOTH

1Φ12 SMOOTH

1Φ12
SMOOTH

1Φ12 SMOOTH

1Φ12 SMOOTH

1Φ12 SMOOTH

1Φ12 SMOOTH

3Φ12
SMOOTH

2Φ12

SECTION B-B

Φ8/10

5Φ12

Specimen IS12XM **(7)**, 2 LAYERS SRP12X (160mm)

Specimen ICM **(8)**, 1 LAYER CFRP (150mm)

Specimen IS3X2M **(9)**
2 LAYERS SRP3X2 (160mm)

Specimen IVS **(10)**

B

3Φ12
S500

SMOOTH
STIRRUPS
O8/20

4Φ16
S500

B

10 | 100 | 100 | 10

200

320

3Φ12
S500 RIBBED

4Φ16
S500 RIBBED

SECTION B-B

3Φ12
S500

20

40

Φ8/20

4Φ16 S500

Specimen IS12XSM **(13)**

Specimen IS3XSM **(11)**

Specimen ICSM **(12)**

Figure 5. Details of the specimens that represent the support region of a continuous beam.

Figure 6. Reaction frame and specimen during test.

Figure 7. Layout of LVDTs on the two types of specimens (instruments are shown on one side only).

Figure 8. Damage patterns in the first group of specimens, representing the span of a continuous beam, after testing.

Figure 9. Load vs. mid-span deflection, for the first group of specimens

Figure 10. Load vs. elongation of the bottom side (at midspan) of the first group of specimens
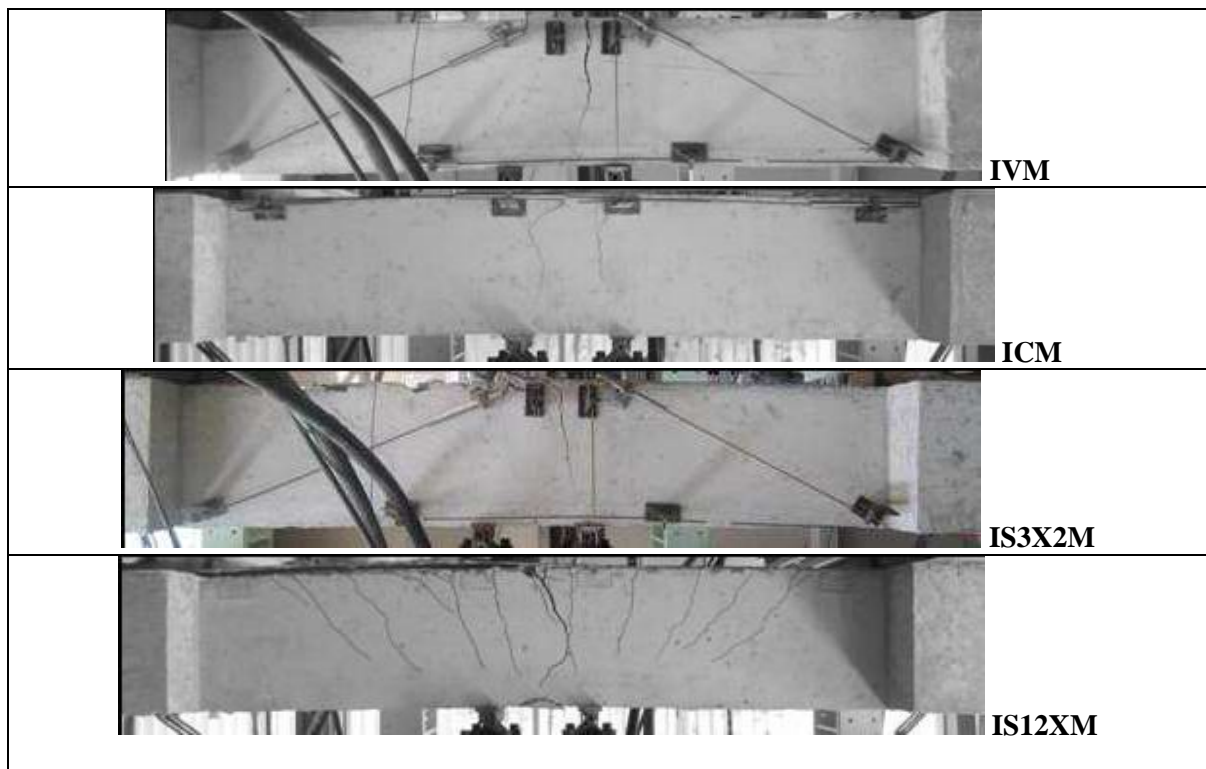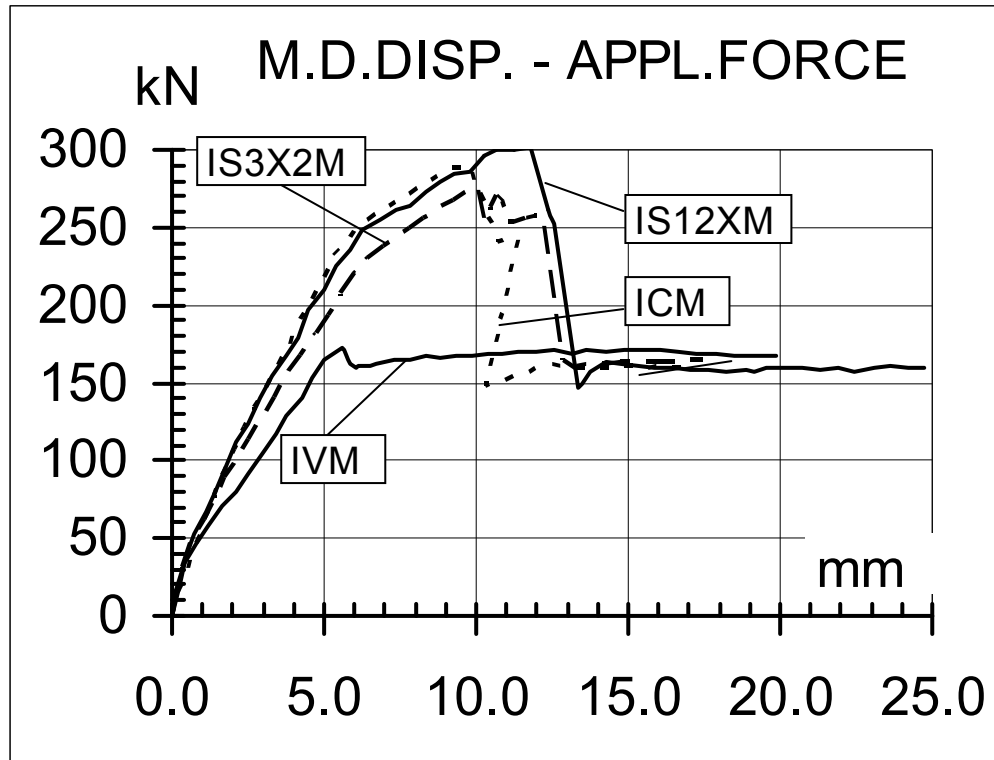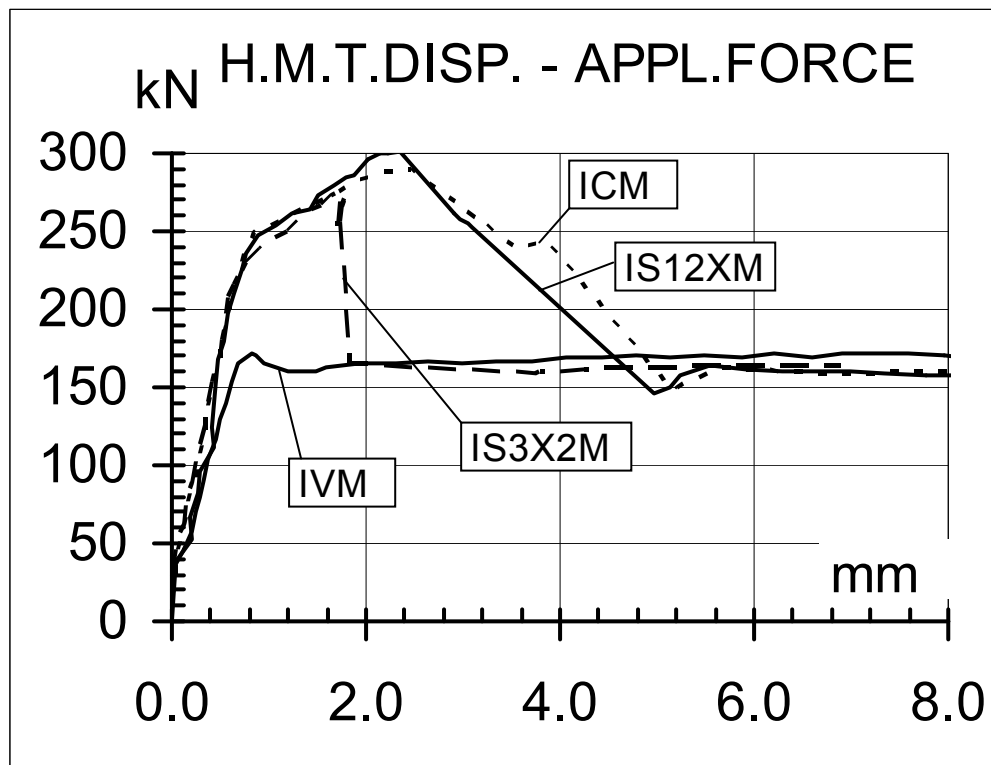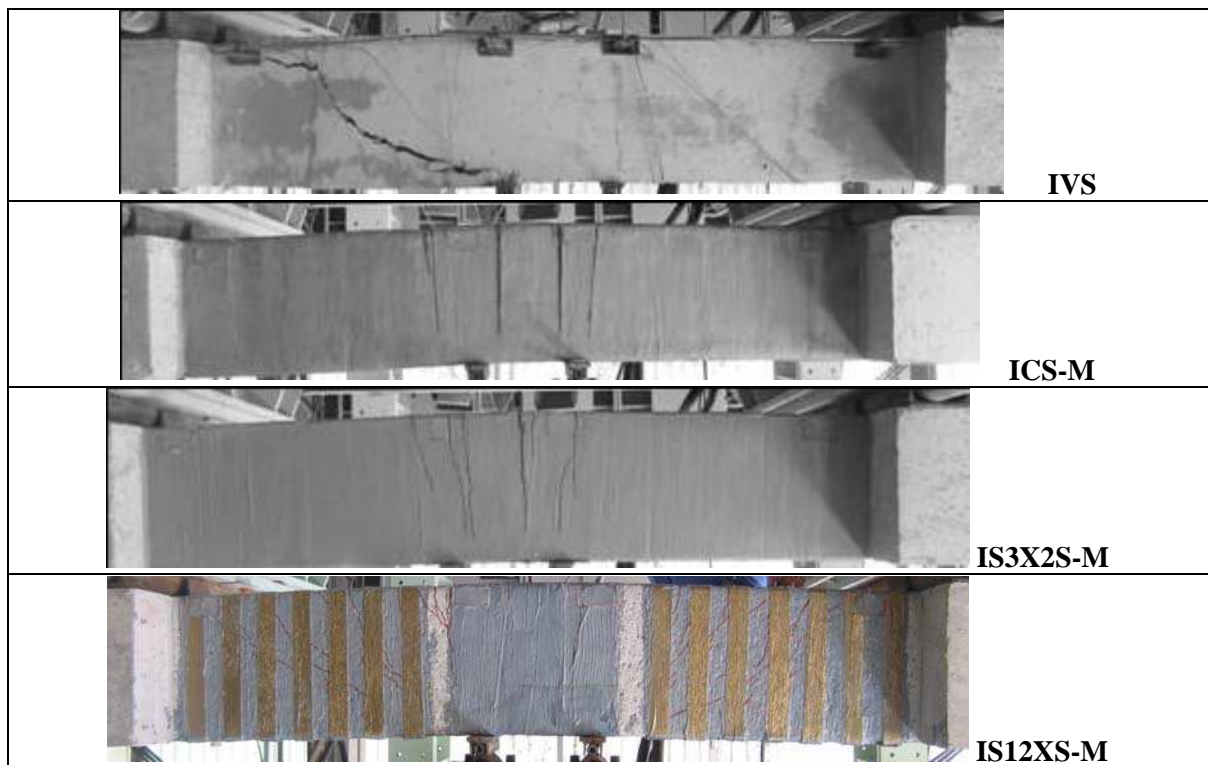
Figure 11. Damage patterns in the second group of specimens representing the support of a continuous beam (flexurally strengthened), after testing (specimens shown upside-down, to better portray the support region of a continuous beam).

Figure 12. Load vs. mid-span deflection, for the second group of specimens

Figure 13. Load vs. elongation of the bottom side (at midspan) for the second group of specimens

Figure 14. Damage patterns in the third group of specimens representing the support of a continuous beam (strengthened in shear), after test (specimens shown upside-down).
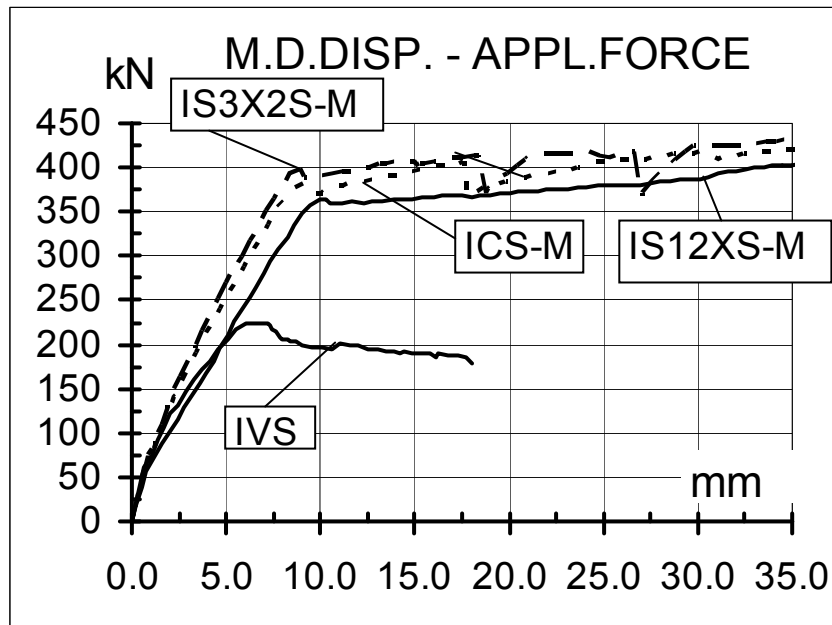
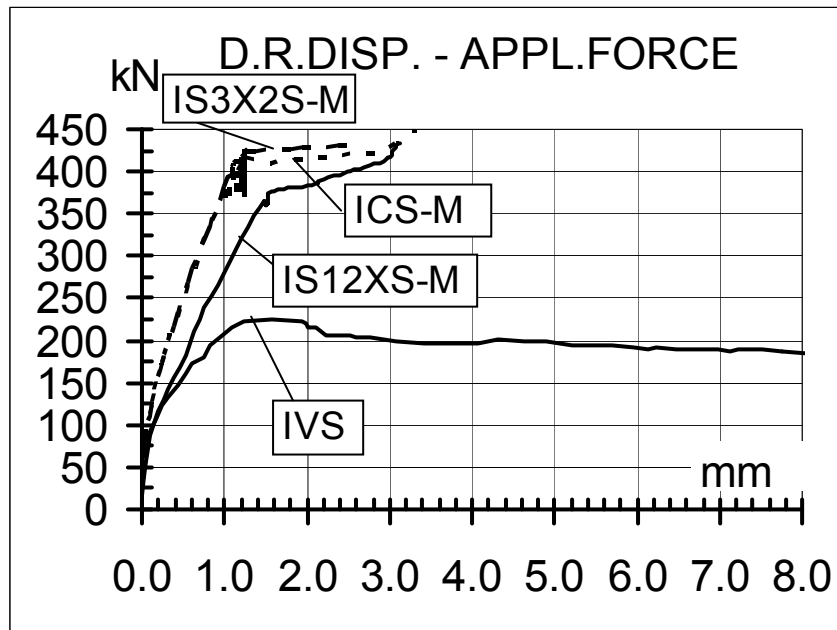Figure 15. Load vs. mid-span deflection, for the third group of specimens

Figure 16. Load vs. diagonal elongation (right side), for the third group of specimens
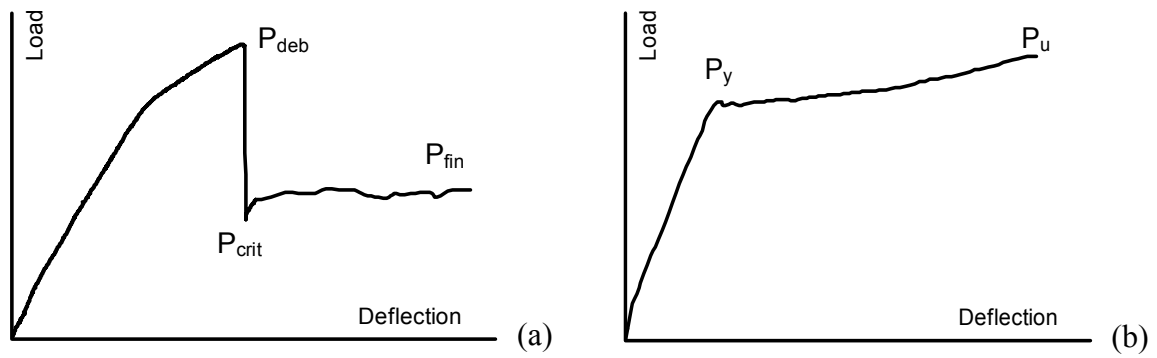
Fig. 17. Typical load – deflection diagrams for:
(a) flexurally strengthened specimens (with debonding)
(b) shear strengthened specimens (no debonding)

Table captions

Table 1. Calculated versus experimentally measured strengths of the specimens

Figure captions

Figure 1. Moment and shear force distribution in the actual continuous beam (upper part) and in the specimens tested, and shear design procedure used (Vconc, Vstir, Vdiag, refer to the shear carried by concrete, stirrups, and bent-up bars, respectively).

Figure 2. Stress – strain diagrams for Ø8 and Ø12 smooth reinforcement bars.

Figure 3. Stress – strain diagrams for Ø12, Ø16 and Ø18 ribbed reinforcement bars.

Figure 4. Details of the specimens that represent the span of a continuous beam.

Figure 5. Details of the specimens that represent the support region of a continuous beam.

Figure 6. Reaction frame and specimen during test.

Figure 7. Layout of LVDTs on the two types of specimens (instruments are shown on one side only).

Figure 8. Damage patterns in the first group of specimens, representing the span of a continuous beam, after testing.

Figure 9. Load vs. mid-span deflection, for the first group of specimens

Figure 10. Load vs. elongation of the bottom side (at midspan) of the first group of specimens

Figure 11. Damage patterns in the second group of specimens representing the support of a continuous beam (flexurally strengthened), after testing (specimens shown upside-down, to better portray the support region of a continuous beam).

Figure 12. Load vs. mid-span deflection, for the second group of specimens

Figure 13. Load vs. elongation of the bottom side (at midspan) for the second group of specimens.

Figure 14. Damage patterns in the third group of specimens representing the support of a continuous beam (strengthened in shear), after test (specimens shown upside-down).

Figure 15. Load vs. mid-span deflection, for the third group of specimens.

Figure 16. Load vs. diagonal elongation (right side), for the third group of specimens.

Figure 17. Typical load – deflection diagrams for: (a) flexurally strengthened specimens (with debonding); (b) shear strengthened specimens (no debonding)